

Scientific Article

Online Prostate-Specific Membrane Antigen and Positron Emission Tomography—Guided Radiation Therapy for Oligometastatic Prostate Cancer



William T. Hrinivich, PhD,^{a,1} Ryan Phillips, MD, PhD,^{a,1}
Angela J. Da Silva, PhD,^b Noura Radwan, MD,^a Michael A. Gorin, MD,^c
Steven P. Rowe, MD, PhD,^d Kenneth J. Pienta, MD,^c
Martin G. Pomper, MD, PhD,^d John Wong, PhD,^a
Phuoc T. Tran, MD, PhD,^{a,c,d,*} and Ken Kang-Hsin Wang, PhD^a

^aRadiation Oncology and Molecular Radiation Sciences, Johns Hopkins Medicine, Baltimore, Maryland; ^bRefleXion Medical, Hayward, California; ^cDepartment of Urology, James Buchanan Urological Institute, Johns Hopkins Medicine, Baltimore, Maryland; and ^dDepartment of Oncology, Sidney Kimmel Comprehensive Cancer Center, Johns Hopkins Medicine, Baltimore, Maryland

Received 12 July 2019; revised 3 October 2019; accepted 11 October 2019

Abstract

Purpose: Stereotactic ablative radiation therapy (SABR) for oligometastatic prostate cancer (OMPC) may improve clinical outcomes, but current challenges in intrafraction tracking of multiple small targets limits treatment accuracy. A biology-guided radiation therapy (BgRT) delivery system incorporating positron emission tomography (PET) detectors is being developed to use radiotracer uptake as a biologic fiducial for intrafraction tumor tracking to improve geometric accuracy. This study simulates prostate-specific membrane antigen (PSMA)-directed BgRT using a cohort from our phase II randomized trial of SABR in men with recurrent hormone sensitive OMPC and compares dose distributions to clinical SABR (CSABR).

Sources of support: This work was supported by a research grant from RefleXion Medical. Dr Hrinivich is funded by RefleXion Medical. Dr Phillips is funded by the RSNA. Dr Tran is funded by Ronald Rose, Joan Lazar, Movember Foundation, Prostate Cancer Foundation, RefleXion Medical; National Institutes of Health/National Cancer Institute (R01CA166348, U01CA212007, U01CA231776 and R21CA223403). Dr Wang is funded by Xstrahl Inc, RefleXion Medical, and National Cancer Institute (R21CA223403, R37CA230341, R01CA240811 and P30 CA006973).

Disclosures: Drs Tran, Phillips, and Hrinivich have consulted for RefleXion Medical. Drs Hrinivich, Tran, and Wang have sponsored research with RefleXion Medical. Dr Da Silva is an employee of RefleXion Medical. Dr Tran reports grants from Astellas Pharm, grants from Bayer Health care, during the conduct of the study. In addition, Dr Tran has a patent Compounds and Methods of Use in Ablative Radiotherapy licensed to Natsar Pharm. Dr Pienta reports grants from Progenics, Inc, during the conduct of the study; personal fees from Cue Biopharma, Inc, outside the submitted work. Dr Rowe reports grants from Progenics Pharmaceuticals, Inc, outside the submitted work. Dr Gorin reports grants, personal fees, and nonfinancial support from Progenics Pharmaceuticals, Inc, during the conduct of the study. Dr Gorin also reports financial support from Nanospectra Biosciences, Inc and nonfinancial support from KOELIS, outside the submitted work. Dr Wong reports grants from Elekta, other from Elekta, grants from Xstrahl, personal fees and other from Xstrahl, outside the submitted work. In addition, Dr Wong has a patent Conebeam computed tomography with royalties paid to Elekta, and a patent SARRP licensed to Xstrahl. Dr Pomper reports other from Progenics Pharma, during the conduct of the study. In addition, Dr Pomper has a patent for the imaging agent with royalties paid to Progenics Pharma.

* Corresponding author: Phuoc T. Tran, MD, PhD; E-mail: tranp@jhmi.edu.

¹ W.T. Hrinivich, R. Phillips, and P.T. Tran contributed equally to this work.

<https://doi.org/10.1016/j.adro.2019.10.006>

2452-1094/© 2019 The Author(s). Published by Elsevier Inc. on behalf of American Society for Radiation Oncology. This is an open access article under the CC BY-NC-ND license (<http://creativecommons.org/licenses/by-nc-nd/4.0/>).

Methods and Materials: A research treatment planning system (RTPS) was used to replan 15 patients imaged with PSMA-targeted ^{18}F -DCFPyL PET/computed tomography and previously treated with CSABR using conventional linear accelerators (linacs). The RTPS models a prototype ring-mounted linac incorporating PET and kilo-voltage computed tomography imaging subsystems and can be used to optimize BgRT plans, as well as research SABR (RSABR) plans, which use the prototype linac without radiotracer guidance. CSABR, RSABR, and BgRT plans were compared in terms of maximum planning target volume (PTV) dose (D_{max}), mean dose to proximal organs at risk (D_{OAR}), conformity index, as well as voxel-wise correlation of dose with PET specific uptake values to investigate possible dose-painting effects.

Results: RSABR and BgRT plans resulted in mean \pm standard deviation increases in D_{max} of $4 \pm 11\%$ ($P = .21$) and $18 \pm 15\%$ ($P < .001$) and reductions in D_{OAR} of $-20 \pm 19\%$ ($P < .001$) and $-10 \pm 19\%$ ($P = .02$) compared with CSABR. Similar target coverage was maintained with conformity indices of 0.81 ± 0.04 ($P < .001$) and 0.72 ± 0.08 ($P = .44$) for RSABR and BgRT compared with 0.74 ± 0.08 for CSABR. Dose and log (specific uptake values) had Pearson correlation coefficients of 0.10 (CSABR), 0.16 (RSABR), and 0.31 (BgRT).

Conclusions: BgRT plans provided similar PTV coverage and conformity compared with CSABR while incorporating underlying PET activity. These results demonstrate feasibility of BgRT optimization enabling online PSMA-targeted, PET-based tracked dose delivery for OMPC.

© 2019 The Author(s). Published by Elsevier Inc. on behalf of American Society for Radiation Oncology. This is an open access article under the CC BY-NC-ND license (<http://creativecommons.org/licenses/by-nc-nd/4.0/>).

Introduction

Prostate cancer remains one of the leading causes of cancer-related death in the United States,¹ with mortality preceded by the development of metastatic disease. It has been proposed that some patients may exhibit an intermediate state between localized disease and widespread metastasis, referred to as oligometastasis, where cancer is confined to a limited number of sites and is potentially curable with metastasis-directed treatments.² Stereotactic ablative radiation (SABR) has been investigated for the treatment of oligometastatic prostate cancer (OMPC), and preliminary evidence suggests that this may be an effective treatment option for multiple metastatic sites³⁻⁹ and may lead to improved overall survival.¹⁰ However, disease control after SABR for OMPC depends critically on the ability to accurately deliver high doses to the tumors while sparing adjacent normal tissues. Prostate-specific membrane antigen (PSMA) is a cell surface protein overexpressed in prostate cancer.¹¹ PSMA-targeted positron emission tomography (PET) using agents, including ^{68}Ga -HBED-CC¹² and ^{18}F -DCFPyL,¹³ has demonstrated high sensitivity and specificity for recurrent prostate cancer¹⁴ and may be ideal for tumor localization for metastasis-directed SABR treatment planning.¹⁵

Biology-guided radiation therapy (BgRT) is currently being developed to directly guide radiation therapy (RT) delivery using PET emission data, thereby overcoming limitations in sensitivity and specificity to cancer of existing anatomic imaging modalities used to guide RT such as x-ray, ultrasound, and magnetic resonance imaging.¹⁶ By incorporating PET detectors with a high-speed ring-mounted linear accelerator (linac), a BgRT approach has been proposed that is able to track PET-avid structures during treatment delivery, thereby compensating for setup uncertainties and internal motion

by directly imaging the tumor. Given potential variability in radiotracer uptake within and between tumors, this BgRT approach is designed to enable the optimization of an intensity modulated radiation therapy (IMRT) plan before treatment delivery based on physician contours and conventional dose-volume histogram (DVH) objectives. The radiotracer data acquired at the time of treatment is then used to reconstruct PET images, which are normalized and used to adjust the machine delivery parameters to target the tumor location. Rapidly reconstructed partial PET images, similar to those used in the present BgRT approach, have previously been shown to provide lung tumor positions within 2 mm under realistic free-breathing conditions.¹⁷ A user-defined mask may also be applied to the reconstructed PET images to prevent the treatment of normal tissues exhibiting nonspecific uptake. This BgRT tumor tracking approach differs from previously proposed emission-guided radiation therapy approaches, which directly targeted coincident gamma rays emitted by radiotracers. The previous emission-guided radiation therapy approach depended critically on consistent and specific radiotracer uptake to dose-paint the target and avoid normal tissues.¹⁸

The purpose of the present study is to describe and evaluate a pretreatment BgRT plan optimization approach making use of simulation computed tomographic (CT) scans and coregistered PET images to optimize machine delivery parameters based on contours and DVH objectives while defining a mapping from normalized radiotracer uptake to dose. When used with the BgRT machine, these plans will enable an online PET-based tracked dose delivery with an average latency of 400 ms. The BgRT machine can also be used in a mode that does not use PET, in which case kilo-voltage fan-beam CT (FBCT) is used for patient set up. BgRT and these research SABR

(RSABR) plans are produced in a cohort of castration-sensitive OMPC patients imaged using ^{18}F -DCFPyL PET/CT as a part of a phase II randomized trial investigating metastasis-directed SABR.¹⁹ The BgRT and RSABR plans are compared with clinical SABR (CSABR) plans produced using standard IMRT optimization in terms of target coverage, dose heterogeneity, conformity, normal tissue dose, and possible dose-painting effects.

Methods

BgRT system

A research treatment planning system (RTPS; version 2017, RefleXion Medical, Hayward, CA) was developed modeling a prototype 6 MV linac with a high-speed binary multileaf collimator (MLC) consisting of 64 leaves mounted to a slip-ring gantry incorporating PET and kilovoltage FBCT imaging systems. The BgRT machine is currently under development. The BgRT machine and RTPS are briefly described here, with further details provided in the supplementary document.

BgRT machine

A schematic of the prototype system is shown in Fig 1, which has been modified from a previously proposed emission-guided linac design.^{17,18} Briefly, the system is designed to enable initial patient setup using FBCT and to

image the tumor using PET before and during treatment delivery. A BgRT plan is optimized before treatment delivery, and the system delivers this plan to the tumor location based on the online PET images. Opposing gantry-mounted PET detectors enable coincident gamma-ray detection during treatment within the current plane of treatment delivery. The gantry completes one revolution per second and can acquire a full “ring” of coincident gamma-rays every 500 ms. The system can reconstruct a partial PET image, which is then used to define beam delivery parameters based on the BgRT plan. A “sliding window” approach is used to reconstruct the partial PET images, using the preceding 500 ms of PET data and updated every 100 ms.

BgRT plan optimization

BgRT plans are produced by optimizing fluence based on contours and DVH objectives using a gradient descent-based approach,²⁰ analogous to an accelerated version of conventional DVH-based IMRT optimization.²¹ Simultaneously, a linear mapping between incident fluence and tumor radiotracer uptake is defined using a coregistered pretreatment PET/CT image, described further in Fig. S1. This mapping allows the system to update machine delivery parameters using the online PET images to provide a tracked dose delivery. During treatment planning, the user also defines a mask surrounding the target to exclude the treatment of normal tissue exhibiting nonspecific radiotracer uptake, referred to as the biology-tracking zone (BTZ). The BTZ is intended to encompass the

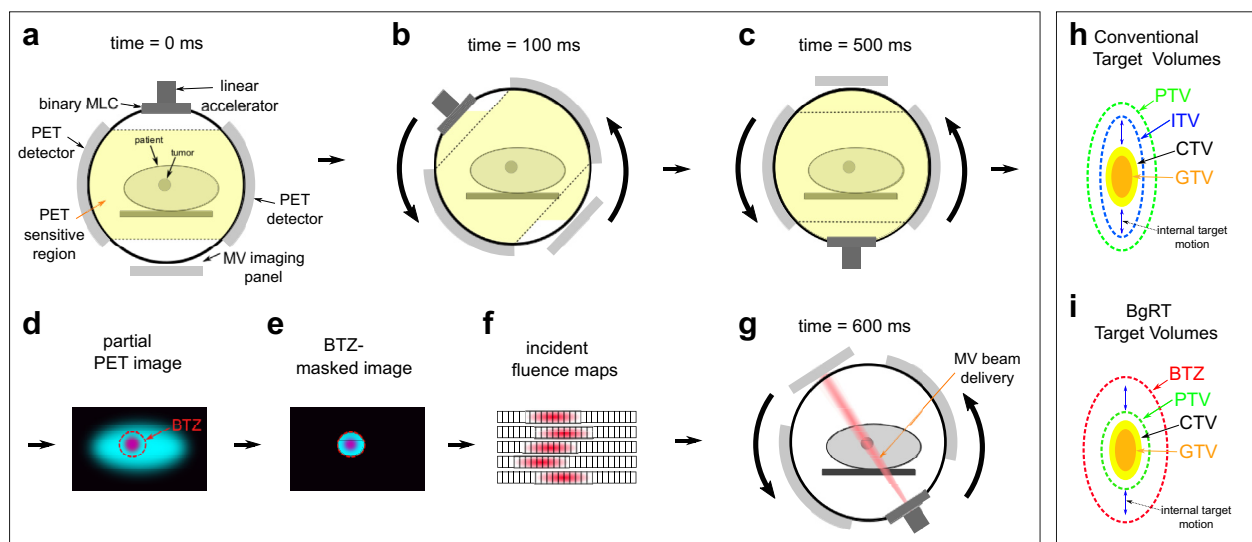


Figure 1 Schematic indicating prototype linac components and biology-guided beam delivery. (a-c) Image acquisition steps, (d-f) image reconstruction and analysis, and (g) beam delivery. (h-i) The difference between standard target volumes and biology-guided radiation therapy (BgRT) target volumes. In both cases, plans are optimized to cover the PTV. The major difference is that the BgRT approach does not require an internal target volume (ITV) to account for internal tumor motion. Instead, internal motion is tracked during delivery within a valid boundary defined by the biology-tracking zone (BTZ). *Abbreviations:* CTV = clinical target volume; GTV = gross tumor volume; PET = positron emission tomography; PTV = planning target volume.

internal motion of the target as illustrated in Fig 1h-i, and is aligned at the start of treatment using FBCT. RSABR plans are optimized using the same algorithm as the BgRT plans, but do not model fluence as a function of PET activity so do not require a pretreatment PET/CT image or a BTZ.

Treatment planning workflow

Fifteen patients were included in this study, selected from the cohort treated with SABR using standard linacs as part of an institutional review board-approved phase II randomized trial of SABR for men with recurrent hormone-sensitive OMPC.¹⁹ A single PET-avid lesion was selected for each patient for replanning using the RTPS. Patient characteristics are summarized in Table 1.

Image acquisition

Patients were imaged for clinical treatment simulation using a Brilliance Big Bore CT scanner (Philips Medical Systems, Cleveland, OH) with 2-mm slice thickness. PSMA-targeted PET/CT was acquired before SABR and at 6 months postrandomization using the radio-labeled PSMA-targeted ligand ¹⁸F-DCFPyL.¹³ PET/CT images were acquired 1 hour after injection using either a Biograph mCT (Siemens, Erlangen, Germany) or Discovery RX (GE Health care, Waukesha, WI) scanner. PET images had isotropic 4-mm voxel dimensions. The initial PET/CT scan was rigidly registered to the simulation CT using Velocity software (Varian Medical Systems, Palo Alto, CA), ensuring optimal registration in the region to be treated.

Clinical treatment planning

CSABR plans were produced using the Pinnacle 9.10 TPS (Philips Medical Systems, Fitchburg, WI) using either volumetric modulated arc therapy (13 cases) or step and shoot intensity modulated radiation therapy (2 cases). Treatments were delivered using either a Synergy linac with Beam Modulator MLC, or a Versa HD linac with Agility MLC (Elekta, Stockholm, Sweden). Normal tissue constraints were selected in accordance with AAPM TG101 guidelines.²² No dose painting techniques were used for CSABR planning. The clinical dosimetrists added structures for plan optimization as needed, typically including concentric shells around the PTV. Six plans did not incorporate a maximum target dose objective, allowing for increased target dose heterogeneity to improve proximal normal tissue sparing.²³ The remaining 9 plans incorporated varying maximum target dose objectives with mean (range) values of 114% (100%-133%) of the prescription dose.

Research treatment planning

RSABR and BgRT plans were produced using the RTPS, beginning with the CT scan, contoured PTV and organs at risk (OARs), prescription dose, and fractionation used for clinical plan optimization. The BTZ structure was produced by applying a 4-mm isotropic expansion to the PTV. Dose shaping structures were produced for all patients including 2 concentric 1 cm thick shells encompassing the PTV or BTZ for the RSABR and BgRT plans, respectively, and an external avoidance structure including the external patient contour and excluding the PTV, BTZ, and shells. Dose

Table 1 Patient characteristics

Patient	No. of metastatic sites	Replanned site	Prescription dose	PTV expansion (mm)	PTV volume (mL)
1	4	Left 5th rib	9 Gy × 3	5	14.4
2	3	Left external iliac node	7.25 Gy × 5	4	24.2
3	4	Left sacroiliac joint	9 Gy × 3	3	19.4
4	1	External iliac node	8 Gy × 5	4	14.2
5	1	Right iliac node	9 Gy × 5	5	9.2
6	2	Left iliac node	9.5 Gy × 3	4	13.3
7	3	Presacral node	7 Gy × 5	5	15.3
8	6	Right iliac node	8 Gy × 5	5	3.2
9	2	Subcarinal node	6.4 Gy × 5	6	21.2
10	2	RP node	9 Gy × 5	5	15.4
11	1	Presacral node	7.25 Gy × 5	5	3.7
12	1	L1 vertebral body	12 Gy × 4	4	6.6
13	1	Left common iliac node	7.25 Gy × 5	6	5.8
14	2	Left internal iliac node	11 Gy × 3	5	8.0
15	1	Sacrum	11 Gy × 3	4	5.3
-	Median (range) 2 (1-6)	-	-	Median (range) 5 (3-6)	Mean (SD) 11.9 (6.6)

Abbreviations: PTV = planning target volume; RP = retroperitoneal; SD = standard deviation.

objectives for optimization were input based on the clinical dose constraints set by the physician. No maximum dose objective was placed on the PTV for all cases. An iterative process was used to optimize dose objectives until acceptable RSABR and BgRT plans were achieved. The RTPS user was not blinded to the clinical treatment plans during optimization and attempted to mimic the trade-offs in PTV coverage and OAR dose where possible to produce a set of comparable plans.

Plan evaluation

Dose metrics

After optimization, CSABR, RSABR, and BgRT treatment plans were exported for analysis using Slicer RT.²⁴ Dose metrics were calculated including the maximum PTV dose (D_{max}), the fraction of the PTV receiving 95% of the prescription dose (V95%), Paddick

conformity index,²⁵ and gradient index.²⁶ The 2 OARs nearest to the PTV were also selected for each patient and used to calculate maximum and mean OAR dose. Maximum and mean doses were expressed as a percentage of the prescription dose for each patient. Dose metrics were compared between planning approaches using repeated measures analysis of variance followed by post hoc paired *t* tests. To investigate the relationship between target and OAR dose, the maximum PTV and OAR doses produced by the RTPS were normalized by the corresponding clinical values. The resultant relative maximum OAR dose was then plotted versus the relative maximum PTV dose, and Pearson correlation coefficients were calculated.

Correlation of dose with PET activity

To investigate the effect of underlying PET activity on the BgRT plans in comparison with the CSABR plans, the dose to each voxel within the PTV from each

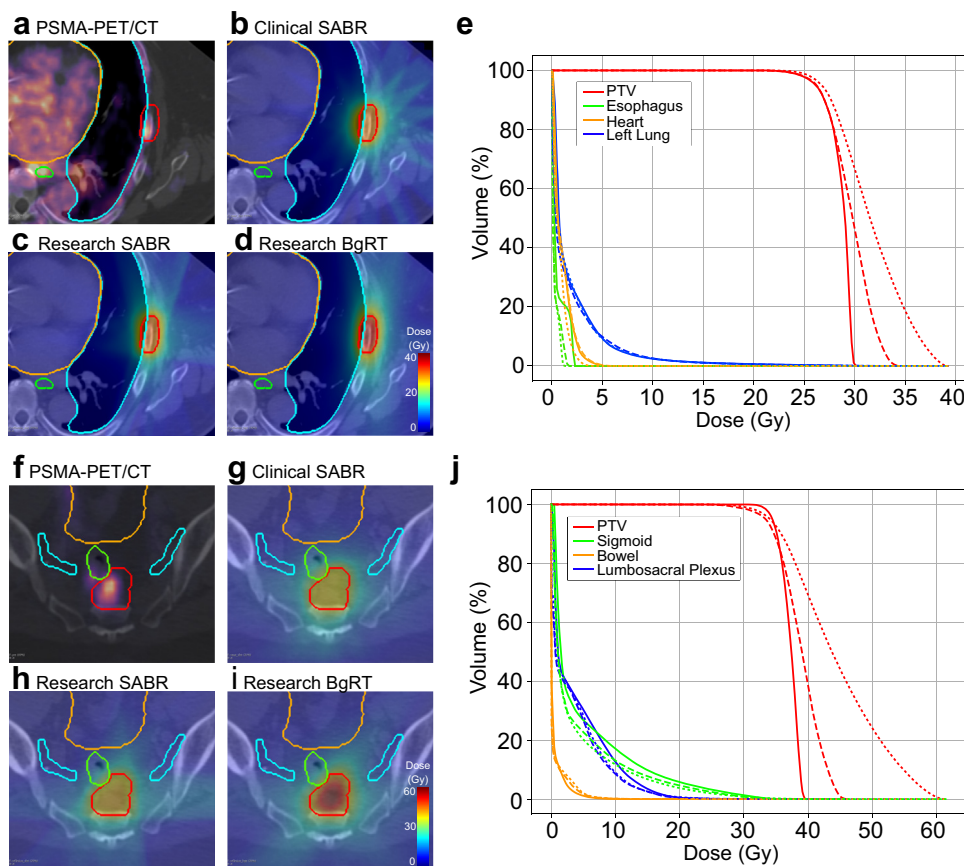


Figure 2 Example images, dose distributions, and cumulative dose-volume histogram (DVH) curves for 2 patients with prescription doses of 27 Gy in 3 fractions (a-e) and 35 Gy in 5 fractions (f-j), respectively. Subfigures include (a, f) prostate-specific membrane antigen/positron emission tomography (PSMA-PET) coregistered with the simulation computed tomography, (b, g) clinical SABR, (c, h) research SABR, and (d, i) biology-guided radiation therapy (BgRT) dose distributions and (e, j) cumulative DVH curves. (e, j) Solid, dashed, and dotted lines correspond to the CSABR, RSABR, and BgRT plans, respectively. Note that the BgRT dose distribution in (i) does not exactly match the PSMA-PET uptake in (f), resulting from the DVH-based plan optimization, which does not directly optimize dose based on radiotracer uptake. *Abbreviation:* PTV = planning target volume.

Table 2 Mean ± standard deviation (*P* value) dose metrics for each planning approach

	PTV D_{max} (% of Rx)	PTV V95%	Conformity index	Gradient index	OAR D_{max} (% of Rx)	OAR D_{mean} (% of Rx)
CSABR	128 ± 11	0.94 ± 0.05	0.74 ± 0.08	4.47 ± 0.63	73 ± 27	11 ± 8
RSABR	133 ± 8 (<i>P</i> = .21)	0.95 ± 0.04 (<i>P</i> = .21)	0.81 ± 0.04 (<i>P</i> < .001)	5.06 ± 0.38 (<i>P</i> = .02)	73 ± 33 (<i>P</i> = .89)	9 ± 8 (<i>P</i> = .001)
BgRT	150 ± 13 (<i>P</i> < .001)	0.95 ± 0.03 (<i>P</i> = .16)	0.72 ± 0.08 (<i>P</i> = .06)	5.40 ± 0.83 (<i>P</i> = .003)	77 ± 35 (<i>P</i> = .06)	10 ± 8 (<i>P</i> = .02)

Abbreviations: BgRT = biology-guided radiation therapy; CSABR = clinical stereotactic ablative radiation therapy; OAR = organs at risk; PTV = planning target volume; RSABR = research stereotactic ablative radiation therapy; Rx = prescription. *P* values are results of post hoc paired *t* tests comparing RSABR and BgRT to CSABR.

planning approach was plotted versus the logarithm of the corresponding PET activity. This analysis was performed at the resolution of the dose grid, which had isotropic 2-mm voxel dimensions for all plans. PET activity was converted to a standardized uptake value (SUV) for each voxel using body weight for semi-quantitative comparison.²⁷ Pearson correlation coefficients were determined between dose and the logarithm of SUV to determine differences between the relationship of dose and PET activity for each planning approach. In addition to voxel-wise analysis of dose versus SUV, the maximum PTV dose was plotted versus the maximum PTV SUV for each patient to determine inpatient effects of variation in PET activity. All statistical analysis was performed using R.²⁸

Results

Dose metrics

Figure 2 shows coregistered CT simulation and PSMA-targeted PET images, planning structures, isodose

lines, and cumulative DVH curves for each planning approach for 2 example patients. Table 2 provides mean ± standard deviation dose metrics for each planning approach along with *P* values from post hoc paired *t* tests comparing RSABR and BgRT to CSABR. Additional statistics are provided in Fig. S1. Target coverage was similar between planning approaches indicated by similar PTV V95% values. In general, target dose heterogeneity was increased when using the RTPS as indicated by the higher D_{max} associated with the research SABR and BgRT plans. RSABR and BgRT plans provided mean ± standard deviation relative increases in D_{max} of 4% ± 11% (*P* = .21) and 18% ± 15% (*P* < .001) compared with CSABR, respectively. Target conformity was highest for the RSABR approach, indicated by statistically significantly higher conformity index values than the CSABR and BgRT approaches. Low-dose bath was increased by the RTPS as indicated by the higher gradient index values. Maximum OAR doses were similar between the RTPS and clinical TPS. Mean ± standard deviation decreases in mean OAR dose were observed for RSABR (−20% ± 19%, *P* < .001) and BgRT (−10% ± 19%, *P* = .02) relative to CSABR.

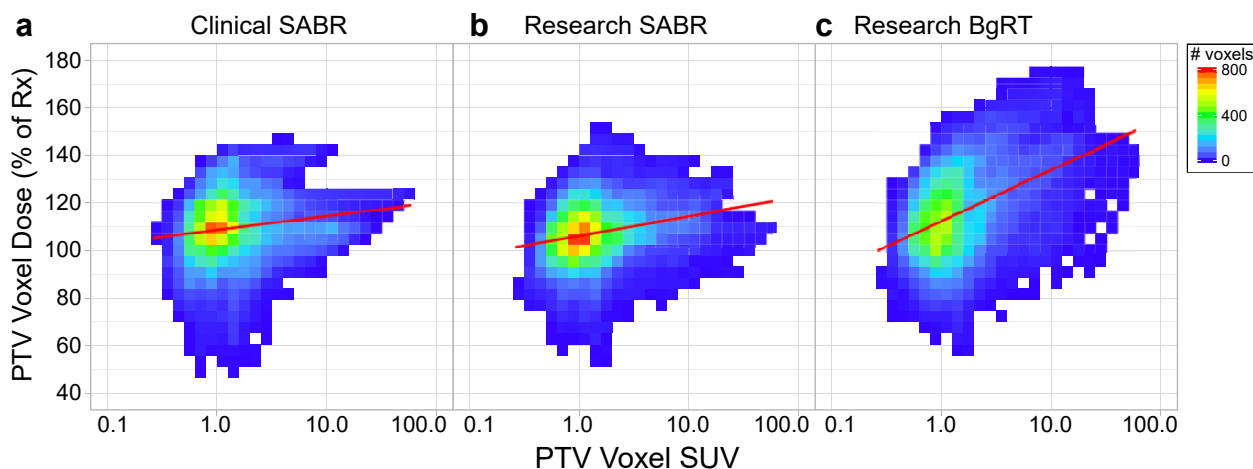


Figure 3 (a-c) Two-dimensional histograms of voxel-wise normalized dose versus the logarithm of standardized uptake value (SUV) for voxels within the PTVs from 15 patients. Lines of best fit are indicated in red. Abbreviations: BgRT = biology-guided radiation therapy; PTV = planning target volume; SABR = stereotactic ablative radiation therapy.

Correlation of dose with PET activity

Figure 3a-c depicts voxel-wise dose as a function of SUV, indicating voxel-wise correlations of dose with underlying PET activity. Pearson correlation coefficients for the CSABR, RSABR, and BgRT plans were 0.10 ($P < .001$), 0.16 ($P < .001$), and 0.31 ($P < .001$), respectively. Figure 4a shows correlation of maximum PTV dose with maximum PTV SUV for each planning approach; Pearson correlation coefficients for the CSABR, RSABR, and BgRT planning approaches were -0.14 ($P = .61$), -0.11 ($P = .69$), and 0.60 ($P = .018$).

Figure 4b shows relative maximum OAR dose versus relative maximum PTV dose for the RSABR and BgRT plans. Maximum OAR dose and maximum PTV dose were not significantly correlated, with Pearson correlation coefficients for the RSABR and BgRT plans of -0.11 ($P = .56$) and -0.16 ($P = .39$), respectively. The majority of points for both approaches were below unity (blue line), indicating a reduction in the ratio of OAR to PTV dose compared with the CSABR plans in most cases.

Discussion

BgRT treatment plans were produced for OMPC patients using PSMA-targeted PET with comparable dose distributions to those achievable clinically while enabling online PSMA-targeted, PET-guided delivery. In particular, similar target coverage between approaches was achieved despite heterogeneous radiotracer uptake within tumors and between tumors in different patients. These plan characteristics are achievable because of the design of the BgRT planning and delivery subsystems. By reconstructing partial PET images during treatment delivery, regions of elevated radiotracer uptake in the target act as biologic fiducials indicating where the dose

distribution should be positioned. The BgRT dose distribution itself is optimized before treatment based on DVH objectives, so does not directly mimic the pattern of radiotracer uptake within the target, enabling the treatment of targets with heterogeneous or partial uptake as illustrated in Fig 2f and 2i. Although not the intended purpose of this BgRT approach, the observed moderate dose-painting effect may provide additional therapeutic benefit relative to CSABR if desired.²⁹ The dose-painting effect may also be mitigated through additional dose objectives on the target not used in this study, such as a homogeneity objective.

Without a homogeneity or maximum PTV dose objective, the BgRT plans resulted in higher maximum PTV doses while decreasing mean dose to the OARs. Increasing target dose heterogeneity is a technique routinely used in stereotactic radiosurgery and standard SABR to improve dose gradients and normal tissue sparing.²² In the present study, 6 CSABR plans also did not incorporate maximum PTV dose objectives; however, the remaining plans incorporated some form of maximum PTV dose objective with varying values and weights. The objectives used for these 9 patients likely contributed to the differences in maximum PTV doses observed between planning approaches. Limiting analysis to the 6 patients without any maximum PTV dose objectives on the CSABR plans, the observed trend remained consistent across planning approaches with mean \pm SD maximum PTV doses of $133\% \pm 13\%$, $136\% \pm 8\%$, and $149\% \pm 18\%$ for the CSABR, RSABR, and BgRT approaches, respectively. However, mean differences with CSABR were no longer statistically significant for RSABR ($P = .37$) or BgRT ($P = .08$) in this small patient subset. The RTOG 0915 guidelines suggests a maximum PTV dose of 167% of the prescription, corresponding to prescribing to the 60% isodose line.³⁰ Three BgRT plans exceeded this constraint, suggesting that clinical implementation of the

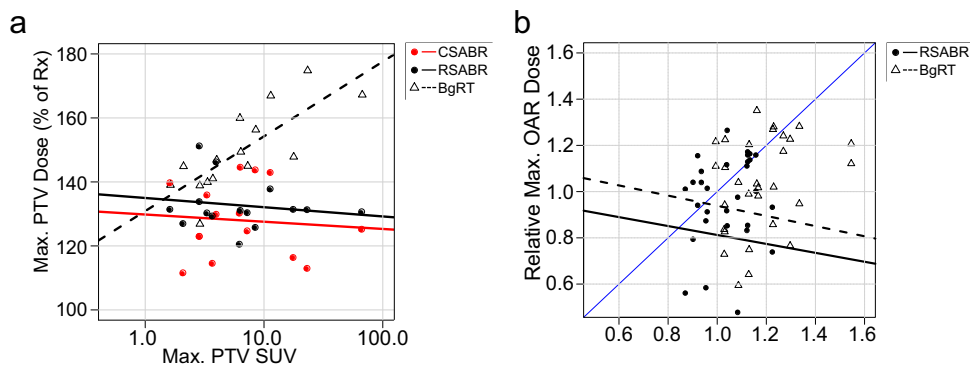


Figure 4 (a) Scatter plots of maximum normalized planning target volume (PTV) dose versus the logarithm of maximum PTV standardized uptake value, with corresponding lines of best fit. (b) Scatter plots of maximum organs at risk (OAR) dose versus maximum PTV dose, both relative to the clinical stereotactic ablative radiation therapy (CSABR) values. The blue identity line (slope = 1) is provided for comparison. *Abbreviations:* BgRT = biology-guided radiation therapy; RSABR = research stereotactic ablative radiation therapy; Rx = prescription.

BgRT technique may necessitate a maximum PTV dose objective in some instances.

The distributions of maximum OAR doses were similar between all 3 planning approaches; however, the RTPS did lead to increased maximum OAR doses in some instances. Specifically, the research dose distributions exceeded clinical constraints more frequently than the CSABR plans, with 4%, 8%, and 10% of constraints exceeded by the CSABR, RSABR, and BgRT plans, respectively. The RTPS tended to decrease mean OAR dose to a greater extent than maximum OAR dose, providing statistically significant improvements in mean OAR dose relative to CSABR. A current limitation of the RTPS is an inability to add additional planning structures within the software after the plan has been initialized, which can be added and used to modulate dose in the clinical TPS. Additional planning structures would enable patient-specific reductions of maximum OAR doses that were not possible in this study.

A major motivation for BgRT is the ability to perform intrafraction tumor tracking using PET, mitigating the effect of internal target motion on treatment uncertainty. This preliminary study did not directly investigate the ability to perform intrafraction tumor tracking using the BgRT approach, but focused on the ability to optimize plans using the RTPS, clinical contours, and coregistered PSMA-PET, which is a prerequisite to BgRT delivery. A prototype linac capable of BgRT delivery has been constructed and is currently being evaluated. Ongoing work involves motion phantom studies investigating the ability to track PET-avid targets during treatment delivery using the prototype system described in this study.

Conclusions

A research TPS has been developed enabling the optimization of BgRT treatment plans using PSMA-targeted PET for OMPC patients. Results suggest that optimized BgRT plans provide similar target coverage and normal tissue sparing compared with conventional SABR plans in the presence of heterogeneous PET tracer uptake, but the BgRT plans did exhibit a moderate metabolism-based dose-painting effect. These plan characteristics indicate that BgRT based on PSMA-targeted PET is feasible for OMPC and may improve clinical outcomes after metastasis-directed SABR.

Supplementary data

Supplementary material for this article can be found at <https://doi.org/10.1016/j.adro.2019.10.006>.

References

1. Siegel RL, Miller KD, Jemal A. Cancer statistics, 2017. *CA Cancer J Clin*. 2017;67:7-30.
2. Hellman S, Weichselbaum RR. Oligometastases. *J Clin Oncol*. 1995;13:8-10.
3. Jerezek-Fossa BA, Beltramo G, Fariselli L, et al. Robotic image guided stereotactic radiotherapy, for isolated recurrent primary, lymph node or metastatic prostate cancer. *Int J Radiat Oncol Biol Phys*. 2012;82:889-897.
4. Schick U, Jorcano S, Nouet P, et al. Androgen deprivation and high-dose radiotherapy for oligometastatic prostate cancer patients with less than five regional and/or distant metastases. *Acta Oncol (Madr)*. 2013;52:1622-1628.
5. Jilg CA, Rischke HC, Reske SN, et al. Salvage lymph node dissection with adjuvant radiotherapy for nodal recurrence of prostate cancer. *J Urol*. 2012;188:2190-2197.
6. Casamassima F, Masi L, Menichelli C, et al. Efficacy of eradication radiotherapy for limited nodal metastases detected with choline PET scan in prostate cancer patients. *Tumori*. 2011;97:49-55.
7. Berkovic P, De Meerleer G, Delrue L, et al. Salvage stereotactic body radiotherapy for patients with limited prostate cancer metastases: Deferring androgen deprivation therapy. *Clin Genitourin Cancer*. 2013;11:27-32.
8. Decaestecker K, De Meerleer G, Lambert B, et al. Repeated stereotactic body radiotherapy for oligometastatic prostate cancer recurrence. *Radiat Oncol*. 2014;9:135.
9. Ameys F, Delrue L, Billiet I, et al. Surveillance or metastasis-directed therapy for oligometastatic prostate cancer recurrence: A prospective, randomized, multicenter phase II trial. *J Clin Oncol*. 2017;36:446-453.
10. Palma DA, Olson R, Harrow S, et al. Stereotactic ablative radiotherapy versus standard of care palliative treatment in patients with oligometastatic cancers (SABR-COMET): A randomised, phase 2, open-label trial. *Lancet*. 2019;393:2051-2058.
11. Sweat SD, Pacelli A, Murphy GP, Bostwick DG. Prostate-specific membrane antigen expression is greatest in prostate adenocarcinoma and lymph node metastases. *Urology*. 1998;52:637-640.
12. Afshar-Oromieh A, Malcher A, Eder M, et al. PET imaging with a [68Ga]gallium-labelled PSMA ligand for the diagnosis of prostate cancer: Biodistribution in humans and first evaluation of tumour lesions. *Eur J Nucl Med Mol Imaging*. 2013;40:486-495.
13. Szabo Z, Mena E, Rowe SP, et al. Initial evaluation of [18F] DCFPyL for prostate-specific membrane antigen (PSMA)-targeted PET imaging of prostate cancer. *Mol Imaging Biol*. 2015;17:565-574.
14. Eiber M, Maurer T, Souvatzoglou M, et al. Evaluation of hybrid 68Ga-PSMA ligand PET/CT in 248 patients with biochemical recurrence after radical prostatectomy. *J Nucl Med*. 2015;56:668-674.
15. Maurer T, Eiber M, Schwaiger M, Gschwend JE. Current use of PSMA-PET in prostate cancer management. *Nat Rev Urol*. 2016;13:226-235.
16. Keall P, Kron T, Zaidi H. In the future, emission-guided radiation therapy will play a critical role in clinical radiation oncology. *Med Phys*. 2019;46:1519-1522.
17. Yang J, Yamamoto T, Mazin SR, Graves EE, Keall PJ. The potential of positron emission tomography for intratreatment dynamic lung tumor tracking: A phantom study. *Med Phys*. 2014;41:021718.
18. Fan Q, Nanduri A, Mazin S, Zhu L. Emission guided radiation therapy for lung and prostate cancers: A feasibility study on a digital patient. *Med Phys*. 2012;39:7140-7152.
19. Radwan N, Phillips R, Ross A, et al. A phase II randomized trial of Observation versus stereotactic ablative RadiatIon for OLigometastatic prostate CancEr (ORIOLE). *BMC Cancer*. 2017;17:453.

20. Beck A, Teboulle M. A Fast iterative shrinkage-thresholding algorithm for linear inverse problems. *SIAM J Imaging Sci.* 2009;2:183-202.
21. Bzdusek K, Friberger H, Eriksson K, et al. Development and evaluation of an efficient approach to volumetric arc therapy planning. *Med Phys.* 2009;36:2328-2339.
22. Benedict SH, Yenice KM, Followill D, et al. Stereotactic body radiation therapy: The report of AAPM Task Group 101. *Med Phys.* 2010;37:4078-4101.
23. Craft D, Khan F, Young M, Bortfeld T. The price of target dose uniformity. *Int J Radiat Oncol Biol Phys.* 2016;96:913-914.
24. Pinter C, Lasso A, Wang A, Jaffray D, Fichtinger G. SlicerRT: Radiation therapy research toolkit for 3D Slicer. *Med Phys.* 2012;39:6332-6338.
25. Paddick I. A simple scoring ratio to index the conformity of radiosurgical treatment plans. Technical note. *J Neurosurg.* 2000;93(Suppl 3):219-222.
26. Paddick I, Lippitz B. A simple dose gradient measurement tool to complement the conformity index. *J Neurosurg.* 2006;105(Suppl):194-201.
27. Li X, Rowe SP, Leal JP, et al. Semiquantitative parameters in PSMA-targeted PET imaging with ¹⁸F-DCFPyL: Variability in normal-organ uptake. *J Nucl Med.* 2017;58:942-946.
28. R Core Team. R: *A language and environment for statistical computing.* 2013.
29. Zamboglou C, Sachpazidis I, Koubar K, et al. Evaluation of intensity modulated radiation therapy dose painting for localized prostate cancer using ⁶⁸Ga-HBED-CC PSMA-PET/CT: A planning study based on histopathology reference. *Radiother Oncol.* 2017;123:472-477.
30. Radiation Therapy Oncology Group. RTOG 0915: A randomized phase II study comparing 2 stereotactic body radiation therapy (SBRT) schedules for medically inoperable patients with stage I peripheral non-small cell lung cancer. *RTOG.* 2009.